Strategies for detecting hydrocarbon microseepages using airborne geophysics integrated with remote sensing data

Julia Barbosa Curto*[1] - julia.curto@gmail.com
Augusto César Bittencourt Pires[1], Adalene Moreira Silva[1] and Álvaro Penteado Crósta[2]

Abstract

Areas affected by light hydrocarbon microseepages present chemical and physical changes in soil, rocks and vegetation. These alterations result in at least six possible indicators which can be effectively detected by airborne geophysics and remote sensing: (i) potassium depletion; (ii) increase of the uranium concentration, in relation to the potassium concentration (DRAD index); (iii) accumulation of magnetic minerals (micromagnetic anomalies); (iv) increase of kaolinite and (v) Fe^{2+} ion concentration; (vi) geobotanic anomalies. This study shows the strategies to identify these typical attributes in some portions of Remanso do Fogo area – MG, using airborne gamma ray spectrometry and magnetic data, integrated with remote sensing data. The geophysical data were applied to detect subtle variations in radiometric and magnetic data by minimizing the influence of recent sediments coverage and deeper magnetic signatures, respectively. Therefore, the gamma-ray spectrometry data were normalized by thorium and yielded low residual potassium and high DRAD values estimates. In the magnetic data, the amplitude of analytic signal of the anomalous magnetic field, using the second derivatives, was the main product to interpret shallow signatures. These magnetic features were related to possible gas pathways. The main geophysical products were integrated using fuzzy logic classification and most potential areas were confirmed by indicators founded in the remote sensing images. Also hydrocarbon iso-concentration curves and known occurrences of microseepages validated the final results.

Introduction

Most of airborne geophysical data used in onshore petroleum exploration was applied to define the basement structural framework. Therefore, the surveys and the technical procedures were typically design to detect deep and regional signatures. With the advance of geophysical researches, the feasibility for the detection of onshore hydrocarbon seepages by geophysical data started to be considered (Saunders *et al*. 1987, 1993; Glenn & Badgery 1998; LeShack & Van Alstine 2002). Parallel to this development, the remote sensing was applied to detect some other important indicators, also provided by hydrocarbon influence (Schumacher & Abrams 1996).

Hydrocarbon microseepage is commonly explained as the result of vertical ascent of colloidal gas bubbles of light hydrocarbons through water filled networks of fractures, joints, and bedding planes within overlying formations (Saunders *et al*. 1999). These paths are affected by physical and chemical changes which result in the formation of the indicators group for the methods used in this study.

Some of these changes are provided by the formation of oxidizing and reduction zones (Saunders *et al*.1993). This process can provide:

a) K depletion;

b) Decrease of U concentration, but not as pronounced as K depletion process;

c) Most Th-bearing minerals stay stable and can be used as a lithological control to define “ideal” and “residual” K and U values;

d) High concentrations of kaolinite;

e) Increase of the Fe^{2+}/Fe^{3+} ratio;

f) Higher concentration of magnetite, maghemite, and iron sulfides, called as micromagnetic anomalies;

g) Geobotanic anomalies.

Accordingly to these indicators presented above, the gamma-ray data were analyzed to detect the variations of K and U, and the magnetic data were used to provide the detection of micromagnetic anomalies and related near-surface geological structures which allowed the percolation of gas to the surface. The remote sensing data were applied to detect high concentrations of kaolinite and Fe^{2+}, as well to identify geobotanic anomalies.

In Brazil, the surveys for this type of application has been mostly based on orbital remote sensing data (Oliveira & Crósta 1996, Augusto *et al*. 2005, Souza Filho *et al*. 2008), whereas magnetometry and gamma-ray spectrometry have been recently considered (Lugão *et al*. 2009).

Therefore, in order to expand the use of indirect methods to map onshore hydrocarbon occurrences, this study shows the results achieved with the use of high-resolution airborne geophysics, composed by gamma-ray spectrometry and magnetometry, integrated with remote sensing data, in the detection of microseepages in the Remanso do Fogo area.

Study Area

This study was developed near and between the junction of Paracatu and São Francisco rivers, located at NW of Minas Gerais state, called Remanso do Fogo area.

This region has a significant amount of gas microseepages (Fugita & Clark Filho 2001), many of them along rivers, lakes and water wells, thus detected by the bubbles that it causes (Oliveira 1998). It also has a history of investigations carried out by Petrobrás since the sixties and stepped out since the nineties by the utilization of direct and indirect prospecting methods, such as surface geochemistry, well logs, geophysics and remote sensing.

The geologic scope of the study area is located in the São Francisco Basin, composed by the Bambuí Group - São Francisco Supergroup - and Sanfranciscana Basin. The mapped lithotypes in the studied area are represented by the Santa Fé de Minas geological map at the 1:100.000 scale (Ribeiro 2003) (Fig.1).

The 1-RF-1-MG well log was made in the study area by Petrobrás in 1992 which provided important information about its stratigraphic profile, estimation of the basin depth, and composition of the hydrocarbons (Fugita & Clark Filho 2001). It has 1848 meter deep, with a stratigraphic section that is composed, from the oldest to the newest unit, as follows: (i) Macaúbas Group, with sandstones and siltstones; (ii) Bambuí Group, with sandstones, siltstones, conglomerate, carbonates, claystones, diamictites and shales; and (iii) Sanfranciscana Basin, with sandstones and siltstones.

Geophysical Processing Methods

This study used the airborne geophysical data from the São Francisco Project – ANP (Brazilian Petroleum National Agency), acquired using north-south line spacing of 500m and orthogonal tie lines spacing of 4,000m at 100m flight height. The data are comprised by gamma-ray spectrometry and magnetic data.

In order to suppress regional contributions, such as geology and weathering process, the Th-normalization technique (Saunders *et al*. 1987, Pires 1995) was applied for the K and U analysis. The gamma-ray spectrometry database was separated according to different types of lithology present in the studied area and regression analysis between K *vs* Th and U *vs* Th associated to each lithology was conducted. Regression equations were used to obtain "ideal" K and U values (Eq.1, Eq.2). Difference between ideal and original concentration values yielded residual K and U estimates (Eq.3, Eq.4).

$$K_i = a + b * Th_S; \quad \textit{(Equation 1)}$$

$$U_i = a + b * Th_S; \quad \textit{(Equation 2)}$$

$$K_{resi} = K_S - K_i; \quad \textit{(Equation 3)}$$

$$U_{resi} = U_S - U_i; \quad \textit{(Equation 4)}$$

Where K_i and U_i are the "ideal" or "predicted" K and U values, K_S , U_S *and* Th_S are the original K, U and Th values, and K_{resi} and U_{resi} are the residual K and U values.

Lower residual potassium values were considered as part of the desired indicators, whereas the residual U values were compared to the residual K values to determine the positive relation U/K. This relationship was calculated using the DRAD index (Saunders *et al*. 1993), Eq.5). Therefore, higher DRAD values were considered as an additional indicator.

$$DRAD = U_{resi} - K_{resi} \quad \textit{(Equation 5)}$$

The procedure used on the magnetic data enhanced the high frequency anomalies, looking for near-surface magnetic features. Therefore, most of the regional information was subtracted from the total magnetic field, resulting on the residual magnetic field. The second derivatives (Dz, Dy and Dx) were used to produce the amplitude of analytic signal, and it was the basis for the interpretation of shallower magnetic responses.

Geophysical Spatial Analysis by Fuzzy Logic

As representatives of near-surface responses, the images of residual K, DRAD and amplitude of analytic signal were integrated using Fuzzy logic classification (Bonham-Carter & Graeme 1994). This process was applied to allow a dynamic observation of different classes of favorability for microseepages. It was produced a classification map using the MS Large fuzzy function in the amplitude of analytic signal and DRAD images, as well the Small fuzzy function was applied in the K residual image (Sawatsky *et al*. 2004). Finally, the resulted products were integrated using the "ADD" Boolean operation.

Remote Sensing Processing Methods

The remote sensing data in this study was provided by the Advanced Spaceborne Thermal Emission and Reflection Radiometer (ASTER). The spectral bands used in this study belong to VNIR (bands 1-3), with 15m spatial resolution, and SWIR (bands 4-9), with 30m spatial resolution.

The Crósta technique (Crósta & Moore 1989, Loughlin 1991) was applied to detect kaolinite concentrations in the studied area. This procedure uses the principal component analysis (PCA) only for the bands which have the desired spectral features. Therefore, it was chosen a band subset comprised bands 1, 4, 5, 6 and 7 for this purpose. The last components of the analysis were selected to produce the kaolinite image.

In order to map Fe^{2+} ion distribution it was used the mineral index by Rowan & Mars (2003) (Eq.6).

$$Fe^{2+} = (ASTER1/ASTER2) + (ASTER5/ASTER3) \quad \textit{(Equation 6)}$$

And the geobotanic anomalies were detected by the application of the NDVI - Normalized Difference Vegetation Index (Rouse *et al*. 1974). Differently from the first two ASTER products, the dark pixels variations in this image were related as interesting regions, because they can represent leaf mass loss or nutritional deficiency caused by the microseepages.

Results

The Remanso do Fogo area is dominated by alluvial sediments and a relatively dense drainage network. These characteristics lead to difficulties in direct identification of areas affected by hydrocarbons and cause the attenuation of near surface geophysical signatures. Therefore, the achieved geophysical results were based on suppressing most of the regional information, emphasizing local signatures.

Normally in regions dominated by sediments coverage and close to fluvial channels, K and U concentrations display already low averages (Dickson & Scott 1997). Because of this, the background suppressing procedure taken to each lithology unit was definitely the main key to find K and U local variations. The application of the Th-normalization technique allowed the detection of the lowest residual potassium values, reflecting local potassium depletion areas and high DRAD values for each lithotype.

The amplitude of the analytic signal showed the nearest surface magnetic features accordingly to the data resolution capability. Almost all the magnetic highs have correspondence with the radiometric results and probably represent the shallower structures of this sedimentary basin portion, which may be controlling the passage of hydrocarbons. It was not possible to discriminate these types of magnetic responses as micromagnetic anomalies; however these zones can be potentially enhanced by the presence of diagenetic magnetite.

Therefore, the application of Fuzzy logic in the near surface geophysical products allowed detecting favorable areas for microseepages occurrences. Most of these areas were validated by hydrocarbon iso-concentration curves and known occurrences of gas. And considering that some of the potential areas are located in portions that were not covered by the geochemical sampling, they may be indicating new microseepages occurrences. Moreover, the irregular distribution of the geochemical sampling causes common displacement errors in the iso-concentration curves, while the geophysical sampling displays a uniform distribution and may be indicating more accurate positions for the hydrocarbon occurrences.

The three ASTER images final products (NDVI, Kaolinite and Fe^{2+}) were analyzed using the pre-defined favorability map, indicated by the geophysical methodology of this study. Most potential areas showed important indicators in the ASTER images.

The brightest pixels are the interest features in the Kaolinite and Fe^{2+} images. It indicates higher concentration of these elements, resulted from the hydrocarbon effects in the environment.

The NDVI image showed the main vegetation domains in the area, such as savannah, gallery forest, and eucalyptus plantation. However it was possible to observe spectral and texture untypical variations inside these domains which are represented by darker pixels and sinuous shapes. It can be indicating leaf mass loss and possible nutritional deficiency features caused by the microseepages.

The meeting of all indicators provided by the integration of the geophysical and remote sensing products allowed the selection of potential areas for microseepages, validated by the geochemical data and known gas occurrences. Three of these areas are illustrated in this manuscript (Figs. 2, 3 and 4), which suggests subsequent detailed investigations.

Conclusions

Due to the availability of geochemical data, the most favorable areas for microseepages evaluated in this study were validated. In addition, other portions of the study area showed analogous potential indicators, suggesting the possibility of new occurrences of light hydrocarbon leak on the surface.

The positive assessment of the presented results has shown the efficiency of the methodology used in this study, allowing its application on other onshore exploration fields. Thus, the essential procedures that provided the indication of potential areas for microseepages in this study were:

a) The thorium-normalized technique applied to the gamma-ray spectrometry data relative to each lithology of the study area allowed the observation of K depletion and its lower values compared to U concentration (DRAD values). Despite the presence of alluvial sediments in a large proportion of the area, this method was very efficient, suppressing most of regional contributions.

b) The amplitude of analytic signal, using the second derivatives, applied to the magnetic data detected near-surface signatures that are represented by possible intra-sedimentary structures and micro-magnetic anomalies. These structures had a significant correspondence with the radiometric anomalies, indicating possible gas paths.

c) The application of Fuzzy logic provided the gathering of all geophysical indicators and the production of a favorability map which showed the potential areas in an easy way of visualization.

d) The ASTER images allowed the addition of other important indicators to the favorable areas indicated by the geophysics, such as high concentration of Kaolinite and Fe^{2+}, and the presence of geobotanic anomalies.

The continuity of this study must focus on checking these potential areas in the field and apply other tools for prospection in greater detail.

Acknowledgments

We thank the contribution of Dr.Wilson de Oliveira; ANP for the permission to use geophysical data for academic purposes; CPRM and CODEMIG for providing the geological map of the region of Santa Fé - MG; LGA/UnB by disposing its infrastructure; CAPES, by granting scholarship to one of the authors; and DPP/UnB, by granting the participation in the congress to one of the authors.

References

Augusto, V.A., Souza Filho, C.R., Almeida-Filho, R., 2005. Caracterização de exsudações de hidrocarbonetos na Bacia do São Francisco-MG por meio de imagens ASTER. In: Congr. Bras. de Sensoriamento Remoto, 12, Goiânia, Anais, p.1733-1740

Bonham-Carter G.F. & Graeme F. (eds.) 1994. Geographic Information Systems for Geoscientists: Modelling with GIS. Pergamon Press, Tarrytown, N.Y., 398p.

Crósta, A.P. & Moore, J.M., 1989. Enhancement of Landsat thematic mapper imagery for residual soil mapping in SW Minas Gerais State, Brazil: A prospective case history in greenstone belt terrain. In: Proceedins of the 7th Thematic Conference on Remote Sensing for Exploration Geology, Calgary, Canada, Environmental Research Institute of Michigan, v. 2, p. 1173–1187.

Dickson, B.L. & Scott, K.M., 1997. Interpretation of aerial gamma-ray surveys-adding the geochemical factors. AGSO Journal of Australian Geology & Geophysics, 17 (2): 187-200.

Fugita, A.M. & Clark Filho, J.G., 2001. Recursos Energéticos da Bacia do São Francisco: Hidrocarbonetos Líquidos e Gasosos. In: Pinto, C.P. & Martins-Neto, M. A. (Ed.), A Bacia do São Francisco. Geologia e Recursos Naturais. SBG/Núcleo MG, p.:265-284.

Glenn, W.E & Badgery, R.A., 1998. High resolution aeromagnetic surveys for hydrocarbon exploration: prospect scale interpretation. Canadian Journal of Exploration Geophysics, 34(1,2): 97-102.

LeShack, L.A. & Van Alstine, D.R., 2002. High-resolution Ground-magnetic (HRGM) and Radiometric Surveys for Hydrocarbon Exploration: Six Case Histories en Western Canada. In: Schumacher, D. & LeShack, L.A. (Ed.), Surface Exploration Case Histories. Applications of Geochemistry, Magnetics, and Remote Sensing. A.A.P.G Studies in Geology N^{o} 48 and SEG Geophysical References Series N^{o}.11, Tulsa, p.: 67-156

Lugão, P.P., Terra, E.F., Maia, M.T.P., Rocha, L.F., 2009.First Magnetic/Gamma Spectrometry Survey for Hydrocarbon Exploration in Brazil Identifies Micro-Seepage Anomalies. 11th International Congress of the Brazilian Geophysical Society, 2009, Salvador.

Loughlin W.P. 1991. Principal component analysis for alteration mapping. Photogrammetric Engineering and Remote Sensing, 57: 1163–1170.

Pires, A.C.B., 1995. Identificação geofísica de áreas de alteração hidrotermal, Crixás-Guarinos, Goiás. Rev.Bras.Geoc., 21(1):61-68.

Rouse, J.W.,Haas, R.H., Schell, J.A., Deering, D.W., Harlan, J.C., (ed) 1974. Monitoring the vernal advancement of retrogradation of natural vegetation. Pasadena: JPL Publication (NASA/GSFC), 151p.

Saunders. D.F., Terry. S. A., Thompson. C. K., 1987. Test of National Uranium Resource Evaluation gamma-ray spectral data in petroleum reconnaissance. Geophysics, 52:1547-1556.

Saunders, D.F., Burson, K.R., Branch, J.F., Thompson, C.K., 1993. Relation of thorium-normalized surface and aerial radiometric data to subsurface petroleum accumulations. Geophysics, 58(10):1417-1427.

Saunders, D.F., Burson, K.R., Thompson C.K., 1999. Model for hydrocarbon microseepage and related near-surface alterations. A.A.P.G.Bull, 83: 170-185.

Schumacher D. & Abrams M.A. (ed.) 1996. Hydrocarbon migration and its near surface expression. A.A.P.G Memoir 66. The American Association of Petroleum Geologists, Tulsa, 441p.

Souza Filho, C.R., Augusto V., Oliveira W.J., Lammoglia T., 2008. Detecção de exsudações de hidrocarbonetos por geobotânica e sensoriamento remoto multi-temporal: estudo de caso no Remanso do Fogo (MG). Rev.Bras.Geoc., 38 (2-suplemento):228-243.

Oliveira, W.J., 1998. Caracterização das Emanações gasosas de hidrocarbonetos na região do Remanso do Fogo (MG) através do uso integrado de sensoriamento remoto, geoquímica, geofísica, geologia estrutural e espectrometria de reflectância. Ph. D. Thesis, State University of Campinas, Brazil, 239p.

Oliveira, W.J. & Crósta, A.P., 1996. Detection of hydrocarbon seepage in the São Francisco Basin, Brazil, through Landsat TM, soil geochemistry and airborne spectrometry data integration. Proccedings of the 17th Thematic Conference and Workshops on Applied Geologic Remote Sensing, Las Vegas, Nevada, vol.1: 155-165.

Ribeiro, J.H., 2003. Belo Horizonte (MG): Projeto São Francisco. SE.23-V-B-VI, mapa geológico, escala 1:100.000. Disponível em: http://www.comig.com.br

Sawatzky D.L., Raines G.L., Bonham-Carter G.F., Looney C.G. 2004. Spatial Data Modeller (SDM): ArcMAP 9.3 Geoprocessing tools for spatial data modelling using weights of evidence, logistic regression, fuzzy logic and neural networks. Disponível em: http:/www.ige.unicamp.br/sdm/ArcSDM3/

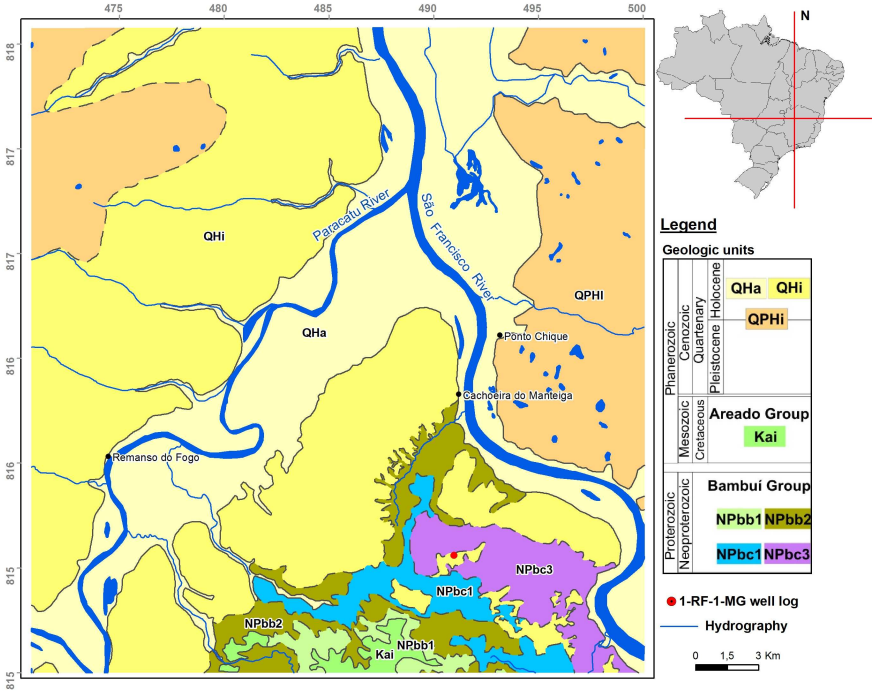

Figure 1 *– Geological map of the studied area, Remanso do Fogo (Ribeiro 2003). Bambuí Group - Lagoa do Jacaré and Serra de Santa Helena Formations: NPbc3: Siltstones with subordinate sandstones and mudstones, often with carbonate cement, and locally, lenses of limestone; and NPbc1: Predominance of calcarenites fine to very fine with subordinated sandstones and siltstones. Bambuí Group – Três Marias Formation: NPbb2: Siltstones associated with arkosean sandstones; and NPbb1: Gray-green arkosean sandstones, siltstones and argillites. Areado Group: Kai - Friable sandstones, with levels of calcitic sandstone and conglomerates. Chapadão Formation: QPHi: Eluvial-colluvial coverage; QHi: Alluvial Terraces; QHa: Alluviums.*

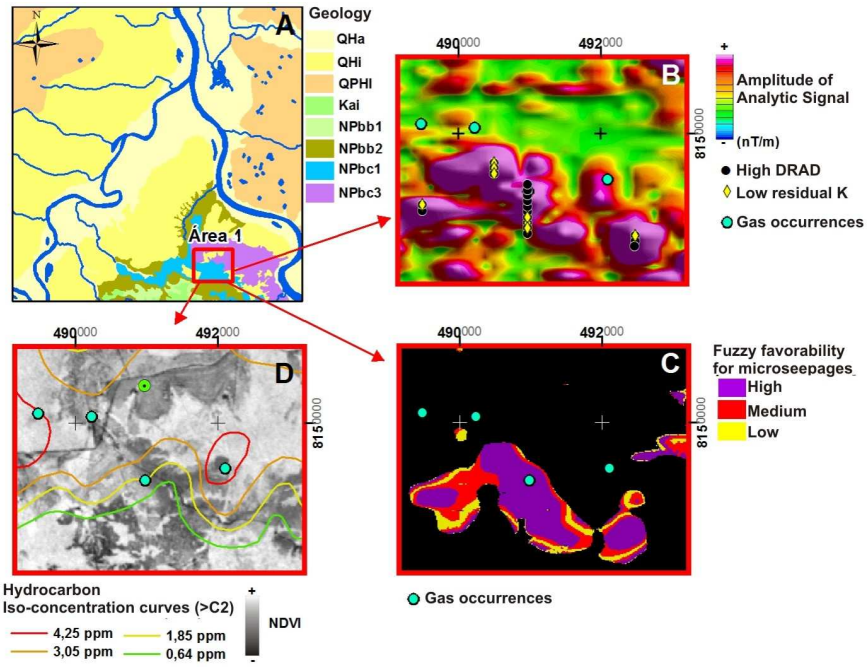

Figure 2 *– Schematic figure outlining the relationship between the indicators for microseepages, validated by the hydrocarbon iso-concentration curves and gas occurrences.* ***A****: Geological map showing the potential area nº 01;* ***B****: high DRAD values and low residual K, overlaid on the amplitude of analytic signal which indicates high magnetic features;* ***C****: classes of Fuzzy favorability for microseepages;* ***D****: NDVI image, where the indicators are comprised by dark pixels.*

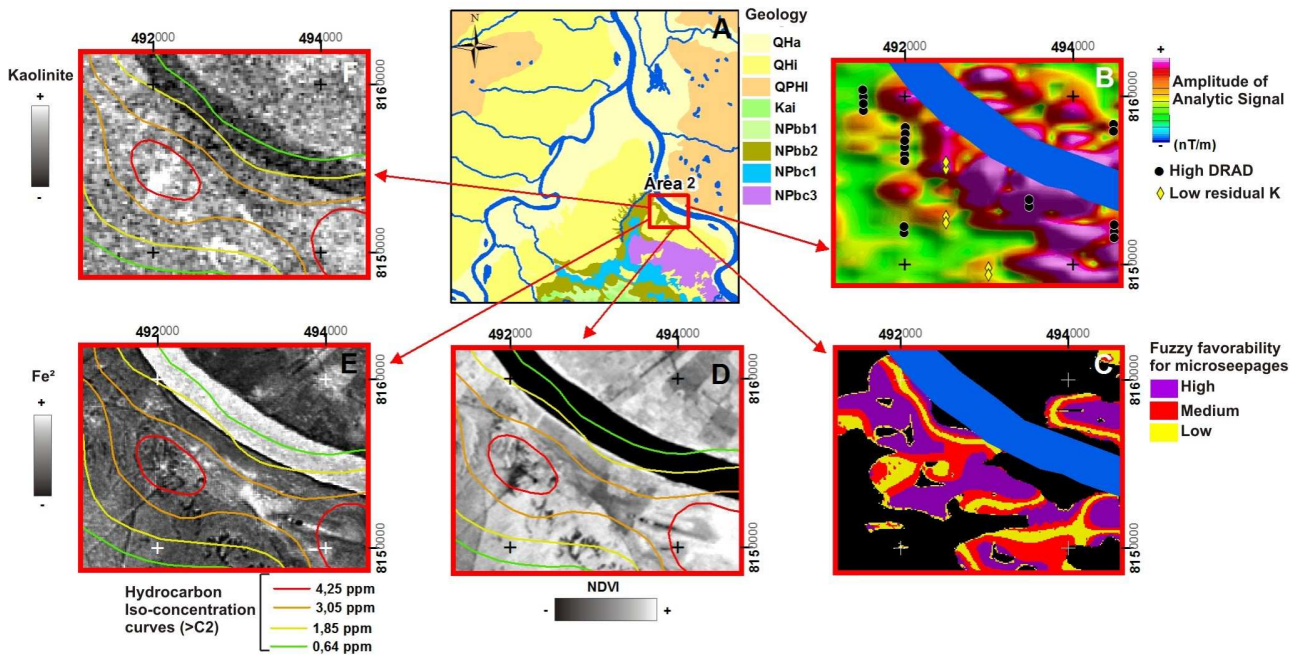

Figure 3 *– Schematic figure outlining the relationship between the indicators for microseepages, validated by the hydrocarbon iso-concentration curves.* ***A****: Geological map showing the potential area nº 02;* ***B****: high DRAD values and low residual K, overlaid on the amplitude of analytic signal which indicates high magnetic features;* ***C****: classes of Fuzzy favorability for microseepages;* ***D****: NDVI image, where the indicators are comprised by dark pixels;* ***E****: Fe^{2+} ion image, where the indicators are comprised by bright pixels;* ***F****: Kaolinite image, where the indicators are comprised by bright pixels.*

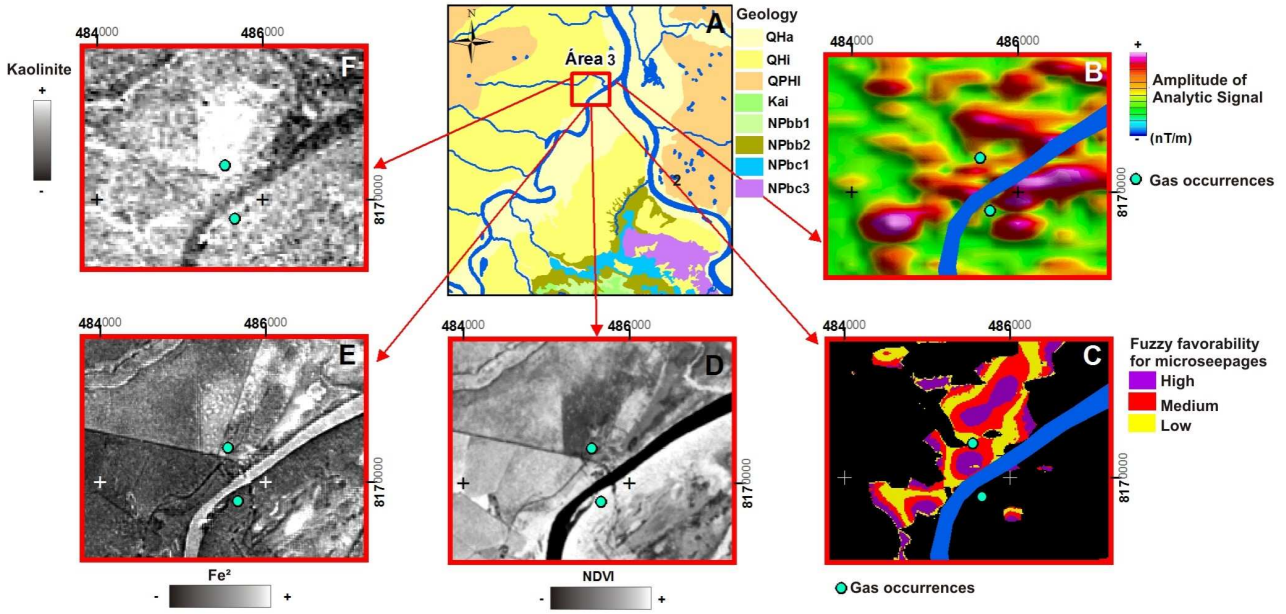

Figure 4 *– Schematic figure outlining the relationship between the indicators for microseepages, validated by the hydrocarbon iso-concentration curves.* ***A****: Geological map showing the potential area nº 03;* ***B****: gas occurrences overlaid on the amplitude of analytic signal which indicates high magnetic features;* ***C****: classes of Fuzzy favorability for microseepages;* ***D****: NDVI image, where the indicators are comprised by dark pixels;* ***E****: Fe^{2+} ion image, where the indicators are comprised by bright pixels;* ***F****: Kaolinite image, where the indicators are comprised by bright pixels.*